

## Adsorption of Tetracycline Hydrochloride from Solutions Using Mesoporous Silica, MCM-48

Paulina Taba\*, Mutmainnah, Yusafir Hala

Department of Chemistry, Faculty Mathematics and Natural Sciences, Universitas Hasanuddin,  
Jl. Perintis Kemerdekaan Km 10, Tamalanrea, Makassar

\*Corresponding Author: paulinataba@unhas.ac.id

Received: November 2020

Received in revised: November 2020

Accepted: December 2020

Available online: January 2021

### Abstract

Mesoporous silica with cubic structure (MCM-48) was synthesized using Ludox HS40 as silica source and cetyltrimethylammonium bromide (CTAB) as a template. MCM-48 was used to adsorb the antibiotic of tetracycline hydrochloride. An X-ray diffractometer observed the x-ray diffraction pattern of MCM-48 and functional groups observed by a Fourier Transformed Infrared (FTIR) spectrometer. Parameters used to study adsorption were contact time and concentration. The pseudo-second-order was the kinetic order that fitted well with the adsorption of tetracycline HCl. The adsorption of tetracycline HCl on MCM-48 followed the Freundlich isotherm with the adsorption capacity of 0.98 mg/g.

*Keywords: MCM-48, antibiotic, tetracycline HCl, adsorption capacity*

### INTRODUCTION

Antibiotics are widely used in humans and animals to cure infections, maintain health and increase animal growth rates (Sapkota et al., 2008, Zhang et al., 2009, Aminov, 2017, Barton, 2000). This function has led to antibiotics receiving particular attention. Also, a specific concern is antibiotic residues in the environment that have continued to develop in recent years (Yang and Carlson, 2017). Antibiotic residues that continuously enter to the environment can cause antibiotic resistance (Yang and Carlson, 2017; Mispagel and Gray, 2005; Fair and Tor, 2014). In 2014 and 2016, several antibiotics were found that were resistant to tuberculosis and malaria (WHO, 2020). Besides, tetracycline antibiotic resistance was also found in *E. Coli* (Karami et al., 2006).

Tetracycline HCl (TCH) is an antibiotic that has a planar structure with four aromatic rings and several functional groups. These functional groups are the tricarbonylamide group, dimethylamino group, and a diketone phenolic group (Gao et al., 2012; Ghadim et al., 2013; Mohammed and Kareem, 2019). TCH antibiotics are included in oral antibiotics obtained from *Streptomyces aureofaciens* (Aminof, 2017; Macsai and Mojico, 2013). The presence of tetracyclines in the aquatic environment was 0.11 µg L<sup>-1</sup> (Boxall, 2004). The, tetracyclines was also found in drainage in Japan (Shimizu et al., 2013).

The presence of antibiotic residues itself occurs due to the low metabolism of antibiotics in the digestive system of humans and animals; about 30%

to 90% of the antibiotics consumed are excreted through the urine and feces as unchanged metabolites or compounds (Kim et al., 2011, Santos et al., 2013, Wang et al. 2019). Therefore, it is essential to develop effective techniques to remove TCH from contaminated waste before discharge to the aquatic environment. Many researchers have tried various methods. These techniques are photodegradation (Khanmohammadi et al., 2020), fenton catalyst for degradation (K), electrocoagulation (Quaissa et al., 2014), electrochemical oxidation (Miyata et al., 2011) and adsorption (Felix et al., 2019, Rizzi et al., 2019, Wang et al, 2020) have been done to solve this problem. Among these techniques, adsorption is considered an effective, cheap, and easy method for removing contaminants (Dehghan et al., 2019).

Adsorption is an effective method to remove contaminants in water and waste (Gao et al., 2012; Mohammed and Kareem, 2019). Recently, adsorption has been widely applied in the removal of antibiotics because it is considered superior to other techniques in terms of flexibility, simplicity of design, cost, and ease of operation (Ghadim et al., 2013, Hao et al., 2012, Marzbali et al., 2016, Nairi et al., 2017., Junyu et al., 2019). One type of adsorbent widely used is mesoporous silica, graphene oxide, glycerol, activated carbon, carbon nanotubes, and chitosan (Ghadim et al., 2013, Zhang et al., Torrellas et al., Wang et al., 2019).

The mesoporous silica of the M4IS group reported in 1992 was named MCM-X (Mobil Crystalline of Materials) (Kresge et al., 1992).

Mesoporous silica is a material that has a high surface area and high pore volume. Also, it has regular pores with a narrow pore size distribution and has high biocompatibility. Mesoporous silica has a pore size of 2-30 nm with a cubic-3D structure, and is one type of mesoporous silica is MCM-48 (Wang et al., 2006). In this study, the synthesis of MCM-48 using Cetyltrimethyl ammonium bromide (CTAB) as surfactants and Ludox HS40 as a silica source was conducted. The antibiotic characterization of MCM-48 is carried out using X-ray Diffraction (XRD) and Fourier Transform Infrared (FTIR). The effect of parameters on TCH adsorption, such as contact time and concentration, was investigated. Langmuir and Freundlich adsorption isothermal models, first-order and second-order pseudo kinetic models were also studied.

## METHODOLOGY

### Materials and Instrumentals

The instrumentals used are an oven (Spin SOSFD type), analytical balance (Ohaus), magnetic stirrer (Fisher Type 115), hotplate stirrer (Ikari Basic 1), vacuum pump (Type ME4C), UV-Vis spectrophotometer (Shimadzu-1800 Series). Prestige-21 FT-IR spectrophotometer, X-ray diffractometer (Shimadzu Maxima-X). The materials used in this study were high purity Merck and Sigma Aldrich. Cetyltrimethylammonium Bromide (CTAB), Ludox HS40, Triton X-100, tetracycline ( $C_{22}H_{24}N_2O_8$ ), acetic acid ( $CH_3COOH$ ), hydrochloric acid (HCl), sodium hydroxide (NaOH), ethanol ( $C_2H_5OH$ ).

### Methods of the MCM-48 Synthesis

Synthesis of MCM-48 was following Ryoo's (1999) procedure with modification of Taba (38). The surfactant was removed from the white product by washing using HCl-ethanol three times. 1 gram of MCM-48 was washed with 25 mL 0.1 M HCl in a 50% ethanol solution while stirring for 30 minutes at room temperature, then filtered. The washing procedure was conducted more than one step; the residue was washed with distilled water and dried at 100 °C.

### Characterization MCM-48

The functional groups of the MCM-48 were analyzed using a Fourier Transform Infrared Spectrophotometer (FTIR). The transmission spectrum is measured in the range from 4000-250  $cm^{-1}$ . XRD measured the X-ray diffraction pattern of MCM-48 powder at a wide-angle ( $2\theta$  range 15-65), the acceleration voltage and applied current were 40 kV and 30 mA, respectively.

### Adsorption of Tetracycline HCl

The antibiotic TCH was used to evaluate the adsorption performance of antibiotics from water by MCM-48. The contact time was investigated by weighing 0.1 g of MCM-48 added in 50 mL of 30 ppm tetracycline solution with a time range of 3-30 minutes. For concentration, 0.1 g MCM-48 is added to 50 mL of the tetracycline solution with a concentration between 10-50 ppm. The whole process is carried out under stirring conditions. The absorbance of tetracycline HCl was measured using UV-Vis spectrophotometer (Shimadzu-1800 Series). The wavelength for this measurement is 276 nm.

The adsorption capacity can be determined using the adsorption isotherm. The isothermal adsorption model used is the Langmuir and Freundlich model. In the Freundlich model,  $\log q_e$  is plotted against  $\log c_e$  and  $c_e/q_e$  against  $c_e$  for the straightforward equation. Intercept the Langmuir equation, the  $k$  value and the Langmuir equation's slope can be obtained the  $q_0$  value related to the adsorption capacity.

## RESULTS AND DISCUSSION

### Characterization using X-ray diffractogram (XRD)

The previous research 2-theta angle below 100 to measure XRD. In this study, mesoporous silica (MCM-48) without washing and after washing with ethanol-HCl was characterized using an XRD device without facilities, for low 2-theta angles. The diffraction pattern of MCM-48 before washing and after washing can be seen in Figure 1.

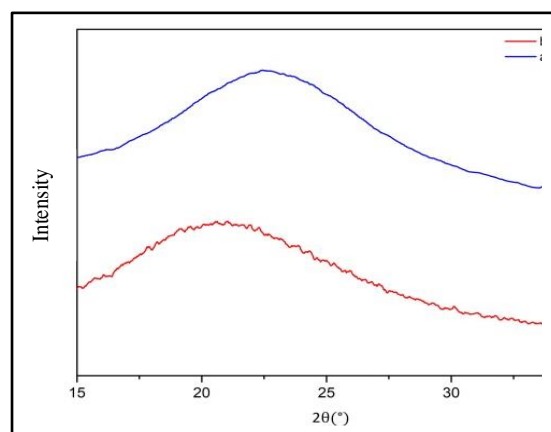


Figure 1. X-ray diffraction pattern of MCM-48 before and after washing

The X-ray diffraction pattern shows intense peaks at 2-theta angles between 20° to 24° and several low-intensity peaks, identical to the study conducted, showed peaks for MCM-48 (Fei et al., 2014). Based

on the results obtained, the material synthesized in this study is MCM-48.

#### Fourier Transform Infrared Spectrometer

Figure 2 shows the MCM-48 spectra before and after washing. The infrared spectrum of MCM-48 before washing, Figure 2a shows the symmetrical stretching vibration of Si-O-Si in the absorption band with a wavenumber of  $795\text{ cm}^{-1}$ . It is supported by the bending vibration of Si-O-Si in the  $451\text{ cm}^{-1}$ . The weak absorption band in  $962\text{ cm}^{-1}$ . Resulted by stretching vibration of Si-O and Si-OH. The strong absorption bands in  $1065\text{ cm}^{-1}$  and  $1229\text{ cm}^{-1}$  are the asymmetric stretching vibrations of Si-O-Si. The stretching C-H vibration is shown in the absorption bands  $1481\text{ cm}^{-1}$  and  $1472\text{ cm}^{-1}$ . The surfactant spectrum's stretching vibration at wavenumber  $2853\text{ cm}^{-1}$  and  $2922\text{ cm}^{-1}$ , indicate symmetric and antisymmetric ( $-\text{CH}_2$ ), respectively. The broad peak at wavenumber  $3441\text{ cm}^{-1}$  shows the stretching vibration of  $-\text{OH}$ . This data is supported by the bending vibration of  $-\text{OH}$  at  $1645\text{ cm}^{-1}$ . These peaks are the contribution of hydroxyl groups and water which are physically adsorbed by MCM-48.

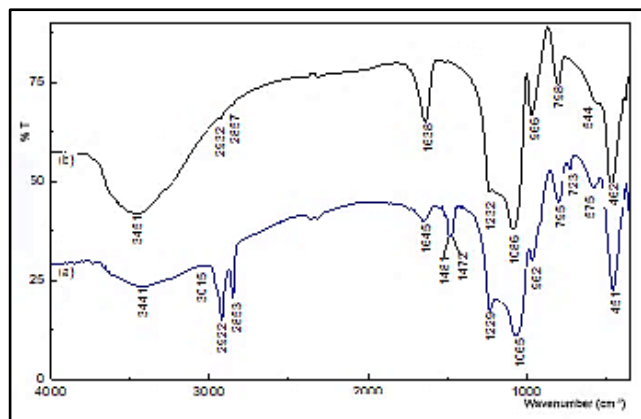


Figure 2. FTIR spectra of MCM-48 (a) before washing and (b) after washing three times with ethanol-HCl

After washing with ethanol-HCl three times (Figure 2b), the stretching and bending vibrations of  $-\text{CH}$  are almost lost. The strong absorption bands at  $1086\text{ cm}^{-1}$  and  $1232\text{ cm}^{-1}$ . The weak ones at  $798\text{ cm}^{-1}$  and  $966\text{ cm}^{-1}$ . This pattern shows the Si-O stretching vibrations from the silicate lattice. After washing by HCl-ethanol solution for three times, the strong peaks at wavenumbers in  $1065\text{ cm}^{-1}$  and  $1229\text{ cm}^{-1}$  shifted by  $21\text{ cm}^{-1}$  and  $3\text{ cm}^{-1}$  due to lattice contraction with surfactant loss. The result according to the previous studies (Chen et al., 1997, Taba et al. 2017, Taba et al., 2018).

#### The surface area Determination by the BET Method

Figure 3 shows the adsorption and desorption of  $\text{N}_2$  gas on MCM-48 before washing and after washing three times. The adsorption isotherm after washing three times is a type d IV isotherm. The MCM-48 curve after washing has hysteresis, which indicates that capillary condensation occurs due to meso-sized particles. The surface area of MCM-48 before and after washing there are  $657\text{ m}^2/\text{g}$  and  $969\text{ m}^2/\text{g}$  respectively. The result shows that the surfactant has been gone, so an inner surface forms after washing and increases the surface area. The pore distribution of MCM-48 before and after washing can be seen in

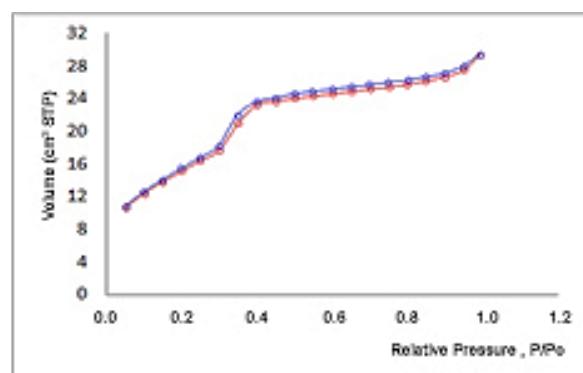


Figure 3. Isothermal  $\text{N}_2$  adsorption after washing three times

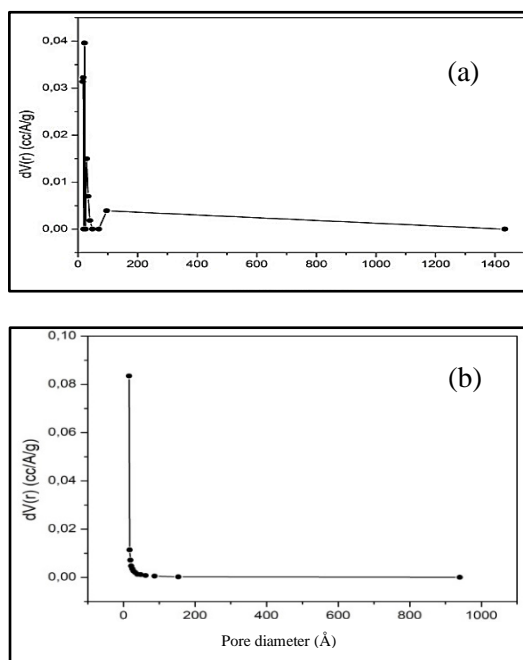


Figure 4. Pore distribution of MCM-48 (a) before washing and (b) after washing for three times

The pore radius according to the BET method for MCM-48 after washing is  $1.52\text{ nm}$  and before

washing is 2.17 nm. So, the pore radius before washing is bigger than after washing. Mean pore radii for MCM-48 after washing (12.18 nm) and before washing (15.38 nm). These data indicate that it has mesoporous sized particles. The total pore volume for MCM-48 after washing is 0.352 cc/g while the total pore volume for MCM-48 before washing was 0.402 cc/g.

### Adsorption of TCH by MCM-48

#### The optimum adsorption time of TCH by MCM-48

The adsorption of TCH increases with the increasing adsorption time until it reaches 20 minutes, they adsorbed tends to decrease. This shows that the adsorption has reached equilibrium at 20 minutes. So the optimum adsorption time is 20 minutes. This time will be used to experiment with variations in pH and concentration.

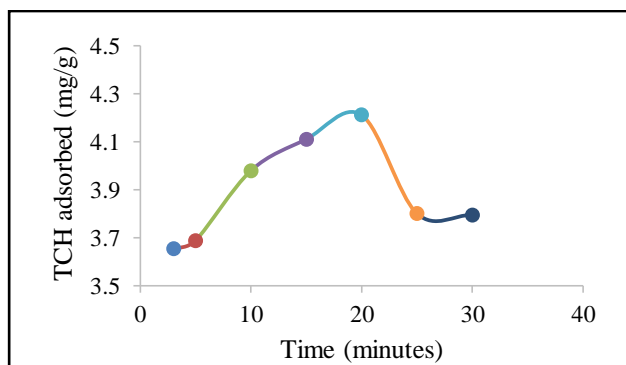


Figure 5 shows the amount of TCH adsorbed by the MCM-48 as a function of contact time.

#### Study of TCH adsorption kinetics by MCM-48

Adsorption kinetics can be studied using pseudo-first-order equations. The differential equation can be seen in Equation 1.

$$\frac{dq_t}{dt} = k_1 (q_e - q_t) \quad (1)$$

where  $q_e$  and  $q_t$  are the amounts of tetracycline HCl adsorbed (mg/g) at equilibrium and at a particular time,  $t$  (minutes),  $k_1$  is pseudo-first-order rate constants ( $\text{minute}^{-1}$ ). The results of the interaction produce Equation 2.

$$\log \frac{q_e}{q_e - q_t} = \log q_e - \frac{k_1}{2,303} t \quad (2)$$

For the pseudo-first-order rate Equation 2 can be written into Equation 3.

$$\frac{dq_t}{dt} = k_1 (q_e - q_t) \quad (3)$$

The rate constant ( $k_1$ ), the adsorption capacity in equilibrium ( $q_e$ ), the correlation coefficient ( $R_1^2$ ) are obtained from the log ( $q_e - q_t$ ) versus  $t$  curve.

The kinetic data can also be processed using pseudo-second-order kinetics models. The differential equation is given by Equation 4.

$$\frac{dq_t}{dt} = k_2 (q_e - q_t)^2 \quad (4)$$

where  $k_2$  is the pseudo-first-order rate constant ( $\text{g/mg}\cdot\text{min}$ ). Integration of equation (4) will result Equation 5.

$$\frac{1}{q_e - q_t} = \frac{1}{q_e} k_2 t \quad (5)$$

Equation 5 can be written in linear form as equation (6) below.

$$\frac{t}{q_t} = \frac{1}{k_2 q_e^2} + \frac{t}{q_e} \quad (6)$$

If pseudo-second-order kinetics are fitted, a plot of  $t/q_t$  versus  $t$  will yield a straight line.

The adsorption kinetics curve for pseudo-first-order and pseudo-second-order can be seen in Figure 6. The  $R^2$  value obtained using the pseudo-first-order kinetics model for TCH adsorption by MCM-48 after washing three times the  $R^2$  value obtained is 0.9839. The  $R^2$  value for the pseudo-second-order kinetics model is 0.999. The  $q_e$  value obtained from the pseudo-first-order kinetics model is 0.98 mg/g and from the pseudo-second-order kinetics model is 4.27 mg/g.

The  $q_e$  value obtained from the experiment is 4.21 mg/g. Although the  $R^2$  obtained from the two models is close to one another, the  $q_e$  from the pseudo-second order kinetics model is close to the  $q_e$  obtained from the experiment. The  $q_e$  obtained from the pseudo-first-order kinetics model is smaller than the experiments. This number shows the adsorption of TCH by MCM-48 after washing three times followed a pseudo-second-order kinetics model with a constant  $k_2$  value of  $0.36 \text{ g}\cdot\text{mg}^{-1}\cdot\text{minutes}^{-1}$ . Debnath et al (2020) also obtained pseudo-second-order kinetics for tetracycline

adsorption on zirconia nanoparticles. Similar results were reported by several researchers using other adsorbents (Yu et al, 2018, Li et al, 2020, Zhang et al, 2020).

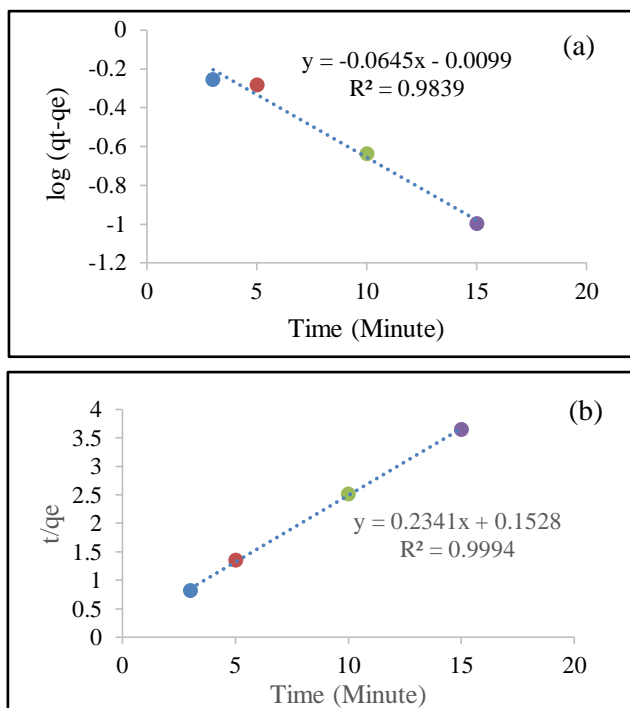


Figure 6. (a) Pseudo-first-order and (b) Pseudo-second-order kinetics models for the adsorption of TCH by MCM-48

#### TCH Capacity by Mesoporous Silica (MCM-48)

Figure 7 shows the amount of TCH adsorbed as a function of the initial TCH concentration. The amount adsorbed increases with increasing initial concentration and so does not show the fixed amount yet at the highest concentration limit used.

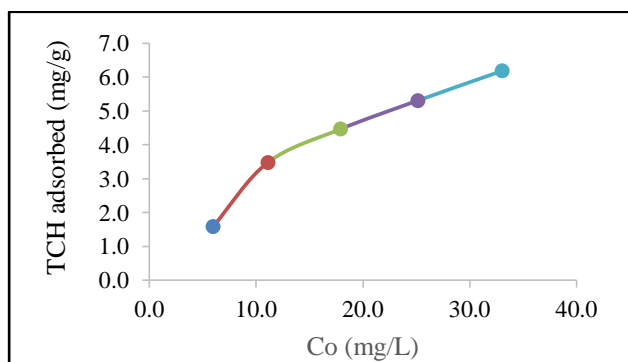


Figure 7. The amount of TCH adsorbed as a function of the initial concentration of the TCH solution

The determining adsorption capacity, the Langmuir and Freundlich isotherms are used. Figure 8 shows the Langmuir and Freundlich isotherms for the

adsorption of tetracycline HCl by MCM-48 after washing three times. Based on the least-squares line ( $R^2$ ) value, the adsorption of tetracycline HCl by MCM-48 after washing three times is more consistent with Freundlich's isotherm ( $R^2 = 0.9475$ ). Based on the Freundlich isotherm, the adsorption capacity obtained is 0.98 mg/g, and  $1/n$  is 0.52. Several researchers also reported Freundlich's isotherm is more suitable for tetracycline adsorption using different adsorbents (Li, 2018, Kong et al., 2020, Prarat, 2020). Generally, the value of  $1/n$  is between 0 and 1, and this value indicates the effect of concentration on the adsorption capacity. The smaller the  $1/n$  number, the better the adsorption performance: generally, for  $1/n$  between 0.1 and 0.5, the substance is easily adsorbed; for  $1/n > 2$ , the compound is difficult to adsorb. The number of  $1/n$  obtained in this study is 0.52, which indicates that the adsorption of tetracycline HCl by MCM-48 is relatively easy (Benkaddour et al., 2019).

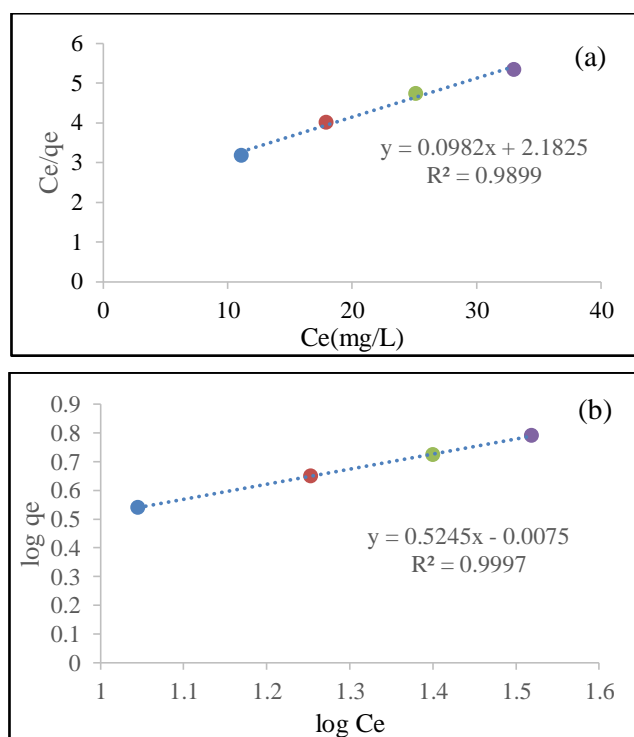


Figure 8. Isotherms (a) Langmuir and (b) Freundlich of TCH adsorption by MCM-48 after washing three times

The amount of tetracyclines adsorbed by MCM-48 after washing three times is lower than other researcher's results (Li, 2018, Kong et al., 2020, Prarat, 2020). This result cause by the surface of the MCM-48 is more polar than the adsorbent used by other researchers. So, the surface of MCM-48 needs to be modified to be more effective in adsorbing TCH.

The absorption peak after adsorption TCH is relatively the same as the absorption peak before adsorption. This pattern shows that the TCH adsorption by MCM-48 is physical adsorption.

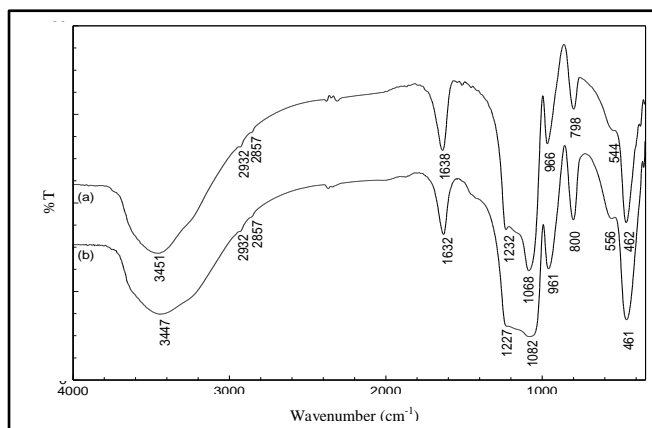


Figure 9. The FTIR spectra before and after TCH adsorption

## CONCLUSION

The adsorption of TCH by MCM-48 reached equilibrium at 20 minutes. The adsorption process fitted in pseudo-second-order kinetics with a rate constant of  $0.36 \text{ g.mg}^{-1}.\text{minute}^{-1}$ . The antibiotic's adsorption fulfils the Freundlich isotherm better than the Langmuir isotherm with an adsorption capacity is  $0.98 \text{ mg.g}^{-1}$ .

## ACKNOWLEDGMENT

The Author, thanks to the Minister of Research and Technology for the Master's research grant obtained.

## REFERENCES

- Aminov, R., 2017. History of Antimicrobial Drug Discovery: Major Classes and Health Impact, *Biochem. Pharmacol.*, 133, 4-19.
- Barton, M.D., 2000. Antibiotic Use in Animal Feed and Its Impact on Human Health, *Nutr. Res. Rev.* 13, 279-299.
- Benkaddour, S., Slimani, R., Hiyane, H., Ouahabi, I.E., and Hachoumi, I., 2018. Removal of reactive yellow 145 by adsorption onto treated watermelon seeds: kinetic and isotherm studies, *Sustain. Chem. Pharm.*, 10, 6-21.
- Boxall, A.B.A., 2004. The Environmental Side Effects of Medication, *EMBO Rep.* 5, 1112-1116.
- Chen, F., Huang, L., and Li, Q., 1997. Synthesis of MCM-48 Using Mixed Cationic-Anionic Surfactants as Templates, *Chem. Mater.*, 9, 2685-2686.
- Debnath, B., Majumdar, M., Bhowmik, M., Bhowmik, K. L., Debnath, A., and Roy, D. N., 2020. The effective adsorption of tetracycline onto zirconia nanoparticlessynthesized by novel microbial green technology, *J. Environ. Manag.*, 261, 110235.
- Dehghan, A., Zarei, A., Jaafari, J., Shams, M. and Khaneghah, A.M., 2019. Tetracycline Removal From Aqueous Solutions Using Zeolite Imidazolate Frameworks with Different Morphologies: A Mathematical Modeling, *Chemosphere*, 217, 250-260.
- Fair, J.R. dan Tor, Y., 2014. Antibiotics and Bacterial Resistance in the 21<sup>st</sup> Century, *Perspect Medicinal Chem*, 6, 25-64.
- Fei, Z., Ai, S., Zhou, Z., Chen, X., Tang, J., Cui, M., Qiao, X., 2014. Enhanced activity of MCM-48 Based Tin Catalyst for Synthesis of 3-Methylbut-3-en-1-ol by Adjusting The Mesochannel Environment, *J. Ind. Eng. Chem.*, 20(6), 4146-4151.
- Felix, A.M.H., Flores, C.A., Cruz, A.M., Barandiaran, J.M, Guzman, S.S. and Silva, R.C. 2019. Removal of Tetracycline Pollutants by Adsorption and Magnetic Separation Using Reduced Graphene Oxide Decorated with  $\alpha\text{-Fe}_2\text{O}_3$  Nanoparticles, *Nanomaterials*, 9, 1-14.
- Gao, Y., Li, Y., Zhang, L., Huang, H., Hu, J., Shah, S.M. and Su, X., 2012. Adsorption and Removal of tetracycline Antibiotics from Aqueous Solution By Graphene Oxide, *J. Colloid and Interface Sci.* 368, 540-546.
- Ghadim, E.E., Manouchehri, F., Soleimani, G., Hosseini, H., Kimiagar, S. and Nafisi, S., 2013. Adsorption Properties of Tetracycline onto Graphene Oxide: Equilibrium, Kinetic and Thermodynamic Studies, *PLoS ONE*, 8, 1-9.
- Hao, R., Xiao, X., Zuo, X., Nan, J., and Zhang, W., 2012. Efficient Adsorption and Visible-Light Photocatalytic Degradation of Tetracycline Hydrochloride Using Mesoporous Bioi microspheres, *J. Hazard. Mater.*, 209, 137-145.
- Junyu, Z., Zefeng, S. and Yuesuo, Y., 2019. Preparation of Low-Cost Sludge Based Mesoporous Carbon and Its Adsorption of Tetracycline Antibiotics, *Water Sci. Technol.*, 79, 676-687.
- Karami, N., Nowrouzian, F., Adlerberth, I. and Wold, A.E., 2006. Tetracycline Resistance in *Escherichia coli* and Persistence in The Infantile Colonic Microbiota, *Antimicrob Agents*

- Chemother*, 50, 156-161.
- Khanmohammadi, M., Shahrouzi, J.R. and Rahmani, F., 2020. Insight into Mesoporous MCM-41 Supported Titania Decorated with CuO Nanoparticles for Enhanced Photodegradation of Tetracycline Antibiotic, *Environ. Sci. Pollut. Res.*, 28, 862–879.
- Kim, K.R., Owens, G., Kwon, S.I., So, K.H., Lee, D.B. and Ok, Y.S. 2011. Occurrence and Environmental Fate of Veterinary Antibiotic in The Terrestrial Environment, *Water Air Soil Pollut.*, 214, 163-174.
- Kong, Y., Zhuanga, Y., Hana, K., and Shi, B., 2020. Enhanced tetracycline adsorption using alginate-graphene-ZIF67 aerogel, *Colloids Surf. A*, 588, 124360.
- Kresge, C.T., Leonowick, M.E., Roth, W.J., Vartuli, J.C. and Beck, J.S. 1992. Ordered Mesoporous Molecular Sieves Synthesized by a Liquid-Crystal Template Mechanism, *Nature*, 359, 710-712.
- Li, M.F., Liu, Y.G., Liu, S.B., Zeng, G.M., Hu, X.J., Tan, X.F., Jiang, L.H., Liu N., Wen, J., and Liu, X.H., 2018. Performance of magnetic grapheneoxide / diethylenetriaminepenta-acetic acid nanocomposite for the tetracycline and ciprofloxacin adsorption in single and binary systems, *J. Colloid Interface Sci.* 521,150–159
- Li, J., Han, J., Meng, F., Jiang, J., Li, J., Xu, C. and Li, Y. 2019. Mesoporous Bimetallic Fe/Co as Highly Active Heterogeneous Fenton Catalyst for the Degradation of Tetracycline Hydrochlorides, *Sci., Rep*, 9, 1-11.
- Li, K., Li, J., Zhao, N., Ma, Y., and Di, B., 2020. Removal of Tetracycline in Sewage and Dairy Products with High-Stable MOF, *Molecules*, 25, 1312
- Macsai, M., and Mojica, G. 2013. *Ocular Surface Disease: Cornea, Conjunctiva and Tear Film*, Elsevier, 1<sup>st</sup> Edition.
- Marzbali, M.H., Esmaili, M., Abolghasemi, H. and Marzbali, M.H. 2016. Tetracycline adsorption by H<sub>3</sub>PO<sub>4</sub>-Activated Carbon Produced from Apricot Nut Shells: A Batch Study, *Process Saf. Environ. Prot.*, 102, 700-709.
- Mispagel, H. and Gray, J.T. Antibiotic Resistance from Wastewater Oxidation Ponds, *Water Environ. Res.* 77, 2996-3002.
- Miyata, M., Ihara, I., Yosida, G., Toyod, K. and Umetsu, K. 2011. Electrochemical Oxidation of Tetracycline Antibiotics using a Ti/IrO<sub>2</sub> Anode for Wastewater Treatment of Animal Husbandary, *Water Sci. Technol.*, 63, 456-461.
- Mohammed, A.A., and Kareem, S.L., 2019. Adsorption of Tetracycline from Wastewater by Using Pistachio Shell Coated with ZnO Nanoparticles: Equilibrium, Kinetic and Isotherm Studies, *Alex. Eng. J.*, 58, 917-928.
- Nairi, V., Medda, L., Monduzzi, M., and Salis, A., 2017, Adsorption and Release of Ampicillin Antibiotic from Ordered Mesoporous Silica, *J. Colloid Interface Sci.*, 497, 217-225.
- Pachauri, P., Falwariya, R., Vyas, S., Maheswari, M., Vyas, R.K., and Gupta, A.B., 2009. Removal of Amoxicillin in Wastewater using Adsorption by Powdered and Granular Activated Carbon and Oxidation with Hydrogen Peroxide, *Nat. Environ. Pollut. Technol.* 8, 481-488.
- Prarat, P., Hongsawat, P., and Punyapalukul, P., 2020. Amino-functionalized Mesoporous Silica-Magnetic Graphene Oxide Nanocomposites as Water-Dispersible Adsorbents For the Removal of The Oxytetracycline Antibiotic from Aqueous Solutions: Adsorption performance, Effects of Coexisting Ions, and Natural Organic Matter. *Environ. Sci. Pollut. Res. Int.*, 27, 6560–6576.
- Quaissa, Y.A., Chabani, M., Amrane, A. and Bensmaili, A., 2014. Removal of Tetracycline by Electrocoagulation: Kinetic and Isotherm Modeling Through Adsorption, *J. Environ. Chem. Eng.*, 2: 177-184.
- Rizzi, V., Lacalamita, D., Gubitosa, J., Fini, P., Patrella, A., Romita, R., Agostiano, A., Gabaldon, J.A., Gorbe, M.I.F., Morte, T.G., and Cosma, P., 2019. Removal of Tetracycline from Polluted Water by Chitosan Olive Pomace Adsorbing Film, *Sci. Total Environ.*, 63, 1-12.
- Santos, L.H.M.L.M., Gros, M., Mozaz, S.R., Matos, C.D., Pena, A., Barcelo, D., and Montenegro, M.C.B.S.M. Contribute of Hospital Effluent to The Load of Pharmaceuticals in Urban Wastewater; Identification of Ecologically Relevant Pharmaceuticals, *Sci. Total Environ.*, 461-462, 302-3016.
- Sapkota, M., Sapkota, A.R., Kucharski, M., Burke, J., McKenzie, S., Walker, P. and Lawrence, R. 2008. Aquaculture Practice and Potential Human Health Risk: Current Knowledge and Future Priorities, *Environ. Int.*, 34, 1215-1226.
- Shimizu, A., Takada, H., Koike, T., Takeshita, A., Saha, M., Rinawati, Nakada, N., Murata, A., Suzuki, T., Chiem, N.H., Tuyen, B.C., Viet, P.H., Siringan, M.A., Kwan. C., Zakaria, M.P., and Reungang, A., 2013. Ubiquitous Occurrence of Sulfonamides in Tropical Asian Water, *Sci. Total Environ.*, 452-453, 108-115.
- Taba, P., Budi, P., and Sari, A.Y.P., 2017. Adsorption

- of Heavy Metals on Amine-Functionalized MCM-48, *Proceeding International Symposium on Current Progress in Functional Materials*, July 26-27, Denpasar Bali
- Taba, P., Mustafa, R.D.P., Ramang, L.M., and Kasim, A.H., 2018. Adsorption of Pb<sup>2+</sup> on Thiol-functionalized Mesoporous Silica, SH-MCM48, *J. Physics, Conference Series*, 979, 012058.
- Torrellas, A.A., Ribeiro, R.S., Gomes, H.T. Ovejero, G., and Garcia, J., 2016. Removal of Antibiotic Compound by Adsorption Using Glycerol Based Carbon Materials, *Chem. Eng. J.*, 296, 277-288.
- Wang, K., Lin, Y., Morris, M.A., and Holmes, J.D., 2006. Preparation of MCM-48 Materials with Enhanced Hydrothermal Stability, *J. Mater. Chem.*, 16, 4051-4057.
- Wang, N., Xiao, W., Niu, B., Duan, W., Zhou, L., and Zheng, Y., 2019. Highly Efficient Adsorption of Fluoroquinolone Antibiotics using Chitosan Derived Granular Hydrogel with 3D Structure, *J. Mol. Liq.*, 281, 307-314.
- Wang, R.Z., Huang, D.L., Liu, Y.G., Zhang, C., Lai, C., Wang, X., Zeng, G.M., Zhang, Q., Gong, M.X., and Xu, P., 2020. Synergistic Removal of Copper and Tetracycline from Aqueous Solution by Steam Activated Bamboo Biochar, *J. Hazard. Mater.*, 384, 1-10
- WHO. 2020. *Antimicrobial Resistance*, World Health Organization.
- Yang, S., and Carlson, K., 2003. Evolution of Antibiotic Occurrence in a River Through Pristine, Urban and Agricultural Landscape, *Water Res.*, 37, 4645-4656.
- Yu, L.L., Cao, W., Wu, S.C., Yang, C., and Cheng, J.H., 2018. Removal of tetracycline from aqueous solution by MOF/graphite oxide pellets: preparation, characteristic, adsorption performance and mechanism, *Ecotoxicol. Environ. Saf.*, 164, 289-296.
- Zhang, X.X., Zhang, T., and Fang, H.H.P., 2009. Antibiotic Resistance Genes in Environment, *Appl. Microbiol Biotechnol.*, 82, 397-414.
- Zhang, Z., Lan, H., Liu, H., Li, H., and Qu, J., 2015. Iron-incorporated Mesoporous Silica for Enhanced Adsorption of Tetracycline in Aqueous Solution, *RSC Adv.*, 5, 42407-42413
- Zhang, Z., Ding, C., Li, Y., Ke, H., and Cheng, G., 2020. Efficient Removal of Tetracycline Hydrochloride from Aqueous Solution by Mesoporous Cage MOF-818, *SN Appl. Sci.*, 2, 1-11.
- Zhao, Y., Geng, J., Wang, X., Gu, X., and Gao, S. 2011. Adsorption of Tetracycline on to Goethite in The Presence of Metal Cations and Humic Substances, *J. Colloid Interface Sci.* 361, 247-251.